Copyright Warning & Restrictions

The copyright law of the United States (Title 17, United States Code) governs the making of photocopies or other reproductions of copyrighted material.

Under certain conditions specified in the law, libraries and archives are authorized to furnish a photocopy or other reproduction. One of these specified conditions is that the photocopy or reproduction is not to be "used for any purpose other than private study, scholarship, or research." If a, user makes a request for, or later uses, a photocopy or reproduction for purposes in excess of "fair use" that user may be liable for copyright infringement,

This institution reserves the right to refuse to accept a copying order if, in its judgment, fulfillment of the order would involve violation of copyright law.

Please Note: The author retains the copyright while the New Jersey Institute of Technology reserves the right to distribute this thesis or dissertation

Printing note: If you do not wish to print this page, then select "Pages from: first page # to: last page #" on the print dialog screen

ABSTRACT

SOOT CAPTURE IN AN ELECTROCATALYTIC REACTOR

by
Thana Slanvetpan

A major problem with many soot emission control devices is the fact that they quickly become loaded with soot which must be removed by a regeneration process. A soot capture reactor using a large flow channel was studied in order to eliminate channel plugging and avoid regeneration. Electrostatic precipitation was used in order to enhance particle diffusion to the catalyst wall of the reactor tube. The system effectiveness for soot capture was measured with filter paper sampling of the incoming versus the outgoing flow through the reactor. Soot filter loadings were analyzed by laser optical transmission. From the soot filter paper samplings combined with a visual inspection of the catalyst material surface, the system effectiveness at low voltages was a combination of the electrostatic precipitation and the catalytic oxidation. Reactor outlet soot concentrations showed a significant decrease when high voltage was applied, showing a strong effect of the electrostatic precipitation. However, catalytic oxidation was not apparent at high voltages because a heavy coating of soot was found on the catalyst surface. Computer simulation models using the Chebyshev Polynomial Software Package were developed to approximate the amount of soot deposited in the reactor tube. The simulation predictions are compared to the experimentally observed soot capture results. The results from this simulation confirmed that the external electric field generated by the use of a central wire has a major effect on the soot capture in the reactor tube.

SOOT CAPTURE IN AN ELECTROCATALYTIC REACTOR

by
Thana Slanvetpan

A Thesis
Submitted to the Faculty of
New Jersey Institute of Technology
in Partial Fulfillment of the Requirements for the Degree of
Master of Science in Chemical Engineering

Department of Chemical Engineering, Chemistry, and Environmental Science

October 1997

APPROVAL PAGE

SOOT CAPTURE IN AN ELECTROCATALYTIC REACTOR

by
Thana Slanvetpan

Dr. Robert Barat, Thesis Advisor — **Date**
Associate Professor of Chemical Engineering
New Jersey Institute of Technology

Dr. John G. Stevens, Committee Member — **Date**
Professor of Mathematics
Monclair State University

Dr. Robert Pfeffer, Committee Member — **Date**
Professor of Chemical Engineering
New Jersey Institute of Technology

BIOGRAPHICAL SKETCH

Author: Thana Slanvetpan

Degree: Master of Science in Chemical Engineering

Date: October 1997

Undergraduate and Graduate Education:

- Master of Science in Chemical Engineering,
  New Jersey Institute of Technology, Newark, NJ, 1997

- Bachelor in Chemical Engineering,
  Chulalongkorn University, Bangkok, Thailand, 1994

Major: Chemical Engineering

The author dedicates this thesis to his parents for their constant inspiration.

ACKNOWLEDGMENT

The author wishes to express his deep sincere gratitude to his advisor, Dr. Robert Barat, for his support, guidance, encouragement, and helpful suggestions. Appreciation is expressed to Dr. John G. Stevens, Professor of Mathematics from Monclair State University for his helpful assistance in the modeling work and a lot of productive suggestions as well as serving as a member of this thesis committee. The author appreciates Professor Robert Pfeffer for his significant comments and serving as a member of the thesis committee. The author would also like to thank PhD candidate, Victor Callahan, for his help and suggestions in the lab.

TABLE OF CONTENTS

TABLE OF CONTENTS
(Continued)

Chapter Page

TABLE OF CONTENTS
(Continued)

Chapter Page

LIST OF FIGURES

Figure Page

CHAPTER 1

INTRODUCTION

1.1 Statement of Problem

Soot has long been recognized as a hazardous pollutant. Due to their small size (smaller than 1 μm), soot particulates can easily enter the human respiratory system. They also often carry polycyclic aromatic hydrocarbons from the combustion process which are known to be carcinogenic; therefore, soot can cause a serious health problem. Soot is also associated with eye irritation and visibility reduction. Soot deposition can cause blockage and corrosion in incinerator units. Furthermore, higher radiative heat transfer caused by abundant soot formation can caused overheating, ultimately damaging the incinerator.

Soot particulates can be separated from the exhaust stream by using a small monolith passage with a catalyst dispersed along the passage surface area. Particles in the bulk flow diffuse and are deposited onto the catalyst surface where soot oxidation takes place. However, the rapid increases in gas pressure drop due to soot accumulation requires frequent filter regeneration or flow bypass. Therefore, several studies of soot control systems have been undertaken.

Soot is primarily a solid particulate composed mainly of carbon. A condensed liquid phase, representing minor fraction of the total particle mass, may be present. The liquid fractions are hydrocarbons resulting from incomplete combustion. They are called soluble organic fractions (SOF), or wet exhaust. These liquid fractions or SOF can volatilize and diffuse into the catalyst pores and oxidize as catalyst temperatures increase. The solid carbon particles in soot are much more difficult to oxidize because the particle is much larger in size than the catalyst pores. It tends to attach itself to the outer flat

surface of the catalyst where there are fewer active sites. Recent studies have suggested that the oxidation of the SOF can sufficiently increase local catalyst temperature to allow part of the solid carbon in soot to be oxidized.

Many of the recent studies in exhaust particulate control have focused on reducing diesel exhaust soot emission. Various concepts have been evaluated to improve the collection and disposal of the diesel exhaust particulate. Some of these will be briefly discussed in the following literature survey.

1.2 Objectives

The objective of this research is to evaluate a catalyst-lined flow reactor, enhanced by electrostatic precipitation, to determine its effectiveness as a soot capture device.

In this research, a reactor using a flow channel larger than that of a small monolith passage was used to eliminate soot plugging. Electrostatic forces were used to enhance particle diffusion to the catalyst wall surface. Variation of voltage in the reactor tube was the primary adjusted operating parameter. A combustion generated soot stream was blown through the electrocatalytic reactor. Toluene was used as the hydrocarbon fuel in this study. The effectiveness of the reactor as a catalytic oxidizer was measured in terms of the soot particle mass density of the incoming versus the outgoing flow through the reactor. In addition, a computer simulation model was developed and compared with the experimental data.

CHAPTER 2

LITERATURE SURVEY

2.1 Catalyst

A catalyst is a substance that affects the rate of a chemical reaction by promoting a different molecular path for the reaction without affecting the chemical equilibrium. Since a catalytic reaction occurs at the fluid-solid interface, a large interfacial area is often helpful or even essential in attaining good conversion. However, extra catalyst surface for an exothermic reaction would merely make a heat-transfer problem more severe. In processes where heat removal is a major consideration, a non-porous catalyst called a monolith is used.

In some cases a catalyst consists of minute particles of an active material dispersed over a less active substance called a support material. The active material is often a pure metal or metal alloy. Such catalysts are called supported catalysts.

Most catalysts do not maintain their activities at the same levels for indefinite periods. They are subject to deactivation, which refers to the decline in the catalyst activity as exposure time progresses. Catalyst deactivation may be caused by an aging phenomenon, called sintering, such as a gradual change in surface crystal structure resulting from the prolonged exposure to high gas-phase temperatures. Poisoning and fouling are the kinds of catalyst deactivation caused by the deposition of a foreign material on active portions of the catalyst surface.

2.2 Soot Control Systems

Many techniques and devices have been developed to reduce or capture the particulate emissions from diesel engine exhaust streams. Some of these techniques focus on engine design such as the combustion chamber and the fuel injection system, the fuel characteristics, and many of the engine operating parameters. Other technologies such as electrostatic precipitation, flow-through catalysts, and particulate traps treat the exhaust to achieve soot reduction.

2.2.1 Filter Traps and Regeneration Systems

Particulate traps such as ceramic filters offer satisfactory soot filtration efficiency. However, the increase in gas pressure drop due to soot accumulation requires frequent filter regeneration. Different methods have been used in order to regenerate particulate traps. These methods can be divided into catalytic and non-catalytic processes. In the former case, fuel additives and catalytic traps have been used. Non catalytic methods often result in complicated and expensive systems.

Thermal oxidation of deposited soot requires relatively high ignition temperatures and a long time for soot to burn out. The process is expensive and result in filter failure due to thermal stress. Oxidation can take place over metal-oxide-based catalysts at much lower temperatures. Therefore, catalytic traps capable of lowering the combustion temperature of the particulate offer an alternative solution.

There are many factors that can influence the catalytic oxidation of soot . In an investigation performed by Ciambelli et al. (1990), oxygen concentration played a substantial role in the oxidation of soot with alumina-supported catalysts containing V,

Cu, and K. The effect of soot concentration was also an important factor. Studies showed that the lower the soot content in the sample stream, the higher the soot conversion.

Ahlstrom and Odenbrand (1990) found that soot combustion took place mainly on the external surfaces of the catalyst. The internal pore surface of the catalyst might be important if desorbed hydrocarbons diffused into the pore structure of the catalyst where combustion could begin. They also found that V_2O_5 was the most active catalyst for the combustion of diesel soot. The study also showed that oxides of Mn and Cr as well as Ag and Pt metal had high activities in the combustion of hydrocarbons that desorbed from the diesel soot.

To prevent the sintering of the active phases, the catalyst is deposited on a thermo-stable support material such as Al_2O_3 or SiO_2 (Yuan et al., 1994). Doorn et al. (1992) found that these support materials were normally inactive in a combustion reactor. Some support materials can act as a catalyst for the combustion of soot. For example, TiO_2 and ZrO_2 have moderate activity, while CeO_2 and $La_2O_2CO_3$ have high activity. The effects of K on TiO_2 supported copper catalysts was also studied by Yuan et al.(1994). The study showed that potassium could stabilize the TiO_2 support texture and increase the surface area of the catalyst.

Cooper et al. (1995) combined a ceramic filter with a catalyst-coated honeycomb converter to make a system called the continuously regenerating particulate trap (CRT). Exhaust fumes passed from the engine into CRT, where they first flowed through a Pt coated ceramic honeycomb. There, CO and NO were catalytically converted to CO_2 and NO_2, respectively. The gas and soot then flowed into a ceramic filter. Instead of clogging the filter, the soot burned in the NO_2 stream to produce CO_2 and N_2 gas. The researchers

claimed that CRT removed 92% of particulates, 96% of hydrocarbons , and 98% of CO from diesel exhausts. The temperature required to induce soot burning was approximately 250 °C, which is sufficiently low to cause no damage to the ceramic filter. However, it cut the engine fuel efficiency by about 2% and, very low-sulfur fuel was required.

As mentioned at the beginning, the ceramic flow monolith is a trap material that can not withstand the thermal shock of rapid regeneration. A new particulate control system was proposed by Khalil and Levendis (1992). Instead of thermal regeneration, which might induce unacceptable thermal gradients and local hot spots within the ceramic monolith filters, the filter was regenerated by a periodically activated flow of compressed air, through the filter element, in the opposite direction of the engine exhaust flow. Particulate blown off the filter were recaptured in a baghouse or burned in a specially designed electric burner.

Using an organometallic additive in the engine fuel is the other solution to reduce the ignition temperature of the particulate during a regeneration cycle (Ludecke and Bly, 1986) It has been found that soot particulates laden with oxides of some metal formulations added to the engine fuel would ignite at a lower temperature than normal particulate.

2.2.2 Cyclone

An alternative to filters for soot removal is a cyclone. Dyson (1989) has produced a simple cyclone that can remove particles of soot and some of the harmful hydrocarbons released in the black exhaust fumes. The particles collected as an oily black mud, a solid cake, or a powder, depending on how cleanly the engine was running. The major advantage of the

device was that it can operate at low temperature. One unexpected advantaged of the cyclone was that it also collected some sulfuric acid, unburned fuel, and harmful aromatic hydrocarbons. Current cyclone designs tend to work best only with moderate gas velocities (Patel, 1991), so further development for fast-moving exhaust is still needed. Particle agglomerators might be needed prior to the cyclone in order to increase the size and mass of the particle to increase cyclone capture efficiency.

2.2.3 Electrostatic Precipitation

An electrostatic precipitator efficiently collects diesel soot particles but does not require regeneration. Studies on electrostatic precipitation were performed by Ludecke (1984) and Dettelson (1986). Electrostatic forces first capture the sub-micron particles on the surface of the trap or agglomerator. After sufficient time, shear forces and other mechanical forces act to reentrain the agglomerated particulates from the surface. The reentrained particles are sufficiently large in diameter so that they could be removed by a relatively simple inertial separation device such as a cyclone. The greatest advantage of using electrostatic precipitation for emission control is that diesel particles are already charged by the combustion process itself. Thus, a simple electrostatic precipitator without a corona section will collect diesel particle efficiently. The absence of a corona is a great advantage over a conventional precipitator because the corona is the main power consumer in an electrostatic precipitator.

Since the electrostatic precipitator does not rely on oxidation of soot particles, the problems with the current regeneration of the trap oxidizers are eliminated. However, maintaining the usual small electrode spacing in these systems might be difficult because of

problems associated with differential thermal expansion. Design of electrically insulated electrode supports that are unaffected by electrically conductive soot is also a major challenge .

CHAPTER 3

EXPERIMENTATION AND EQUIPMENT

3.1 Experimental Schematic

The schematic diagram of the system is shown in Figure 3.1. The system can be separated into two major portions: combustion section and electrocatalytic reactor. The combustion section includes a feed section, the combustor, and a cooling section. The elbow connects the cooling section to the electrocatalytic reactor. The bypass channel reduces the flow rate of the gas stream into the reactor tube to allow enough residence time for soot capture to be achieved. Sampling sections are installed upstream and downstream of the reactor in order to determine the effectiveness of the electrocatalytic reactor. The details for each section are described below.

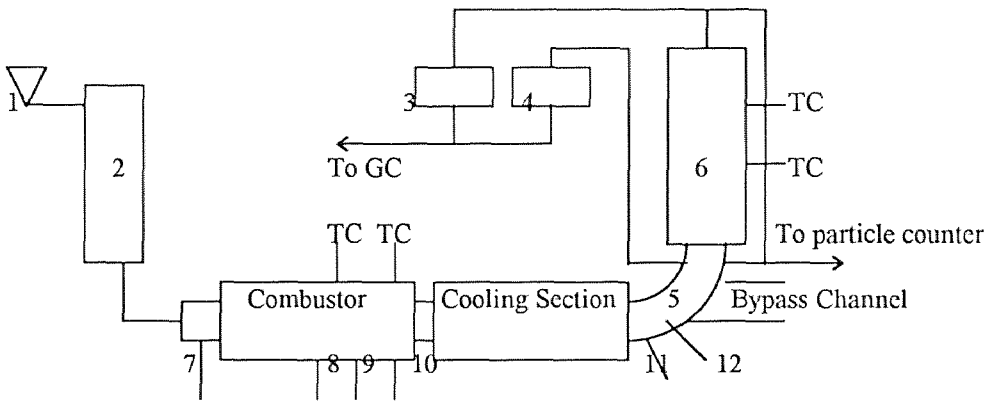

1. Toluene Feeding Section
2. Toluene Tank
3. Outlet Sampling Section
4. Inlet Sampling Section
5. Elbow
6. Electrocatalytic Reactor
7. Air in
8. Ignitor
9. H_2 in
10. N_2 flush line
11. SOF in
12. Liquid N_2 in

Figure 3.1 Experimental Schematic

3.1.1 Toluene Feeding Sections

Toluene is the fuel used in this study because of its good sooting tendency. There are two feed sections in the system. The first section services the primary combustor. The toluene tank was pressurized by nitrogen gas to 110 psig.. The toluene was injected as a liquid fuel spray into a combustor at a rate of 20-22 cc/min. The other feed section is located right at the exhaust elbow. This toluene was added as a vapor directly into the elbow as a soluble organic fraction (SOF) and mixed with the soot stream from the post-combustor cooling section. The SOF toluene was kept in a saturation bubbler located in a constant temperature bath.

3.1.2 Combustor Section

The combustor is comprised of a refractory alumina tube with an inside diameter of 3.25 inches and surrounded by a stainless steel outer tube. The combustor was operated at an overall equivalence ratio (ϕ) about 1.35, and at atmospheric pressure. The overall equivalence ratio (ϕ) is a ratio of the actual molar fuel-to-air ratio to the stoichiometric fuel-to-air ratio. The fuel flowed through a high pressure nozzle to produce a fine spray mist. The fuel flow rate was around 20-22 cc/min. with a pressure of 110-120 psig. Only swirl air was used to burn the toluene. Two thermocouples are provided along the length of the combustor. Typical operating temperatures were in the range of 1400-1600 °C. A cooling coil was wrapped around the outer stainless steel combustor tube to prevent overheating. A nitrogen gas flush line was available for emergency shutdowns.

3.1.3 Cooling Section

The cooling section is located right after the combustor to cool the soot-laden exhaust gas down to about 370 °C. An annular water jacket provided the heat transfer. Additional cooling of the exhaust in the elbow section was achieved by spraying in liquid nitrogen. The cooled exhaust was separated into two flows. The first one went upward into the electrocatalytic reactor. The latter stream went into the bypass channel which was connected straight to the hood. The object of the bypass channel was to adjust and control the amount of flow which went into the electrocatalytic reactor.

3.1.4 Electrocatalytic Reactor

The electrocatalytic reactor, which is the main focus of this research effort, consists of a 17 inch long tube, which has an inside diameter of 1 inch, with a catalyst mesh rolled to form the inside tube surface. The catalyst is an electrically grounded, flat stainless steel sheet coated on one side with alumina support material at 30 mg/in^2 and platinum at 0.5 mg/in^2. A center wire runs down the tube axis and was electrical charged using a DC power supply. The central wire was enclosed with insulated posts. However, a tendency for soot build up on the posts can result in an electrical short circuit. This condition was minimized by operating at a lightly sooting condition or with an equivalence ratio (ϕ) less than 1.4. The temperature of the reactor was regulated by a three-zone temperature controller. Thermocouples were installed along the length of the reactor in order to measure the axial temperature profile.

In order to study the oxidation reaction on the catalyst surface in the electrocatalytic reactor, a specific flow of pure oxygen gas was injected at the entrance of

the reactor. Additional O_2 was required since the fuel-rich feed condition in the combustor limited available O_2 for soot burnout. For reference runs without additional oxygen, nitrogen gas was injected at the same flow rate at the entrance of the reactor tube.

3.1.5 Sampling Sections

The diagrams of the sampling sections are shown in Figures 3.2. and 3.3. All the sample lines used in this study are stainless steel. Sample streams were collected both upstream and downstream of the reactor. A 0.45 μm (pore size) metricel membrane filter (filter paper) was placed in the filter holder, which was placed in-line for each sample line. The collection time for each sample was 10 minutes. As shown in Figure 3.2 and Figure 3.3, a pair of parallel filters for each inlet and outlet sampling line was used. One filter was sacrificed catching soot which had accumulated in the sampling line when the vacuum pump was first activated. The sample line for the upstream sample was water cooled before the sample stream entered the filter.

Soot mass density in the gas was obtained by weighing the filter papers before and after each experiment. In addition, an optical technique was used (described later). By knowing the weight gain of the filter paper and volumetric flow rate of the sampling gas as well as the sampling time, soot mass density in the flow can be determined by the following expression:

Mass density = Weight gained / (sampling flow rate × sample time)

A cooling coil and a water trap were used in the sample line leading to the isokinetic diluter, upstream of the particle counter, in order to cool the sample down and trap the condensed water, respectively.

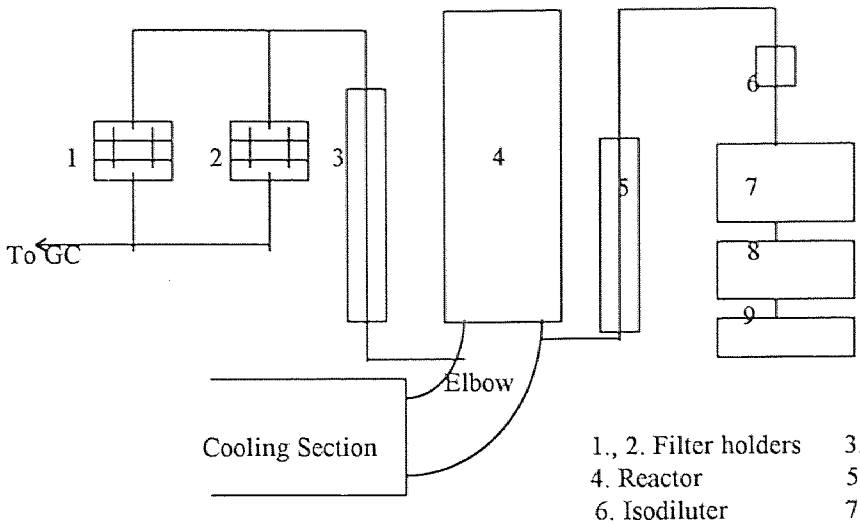

1., 2. Filter holders
3. Cooling Section
4. Reactor
5. Condensate Trap
6. Isodiluter
7. Particle sensor
8. Particle counter
9. On-line printer

Figure 3.2 Inlet Sampling Sections

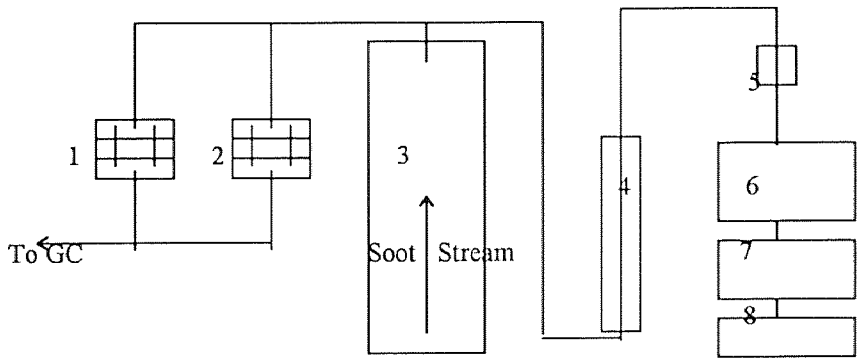

1., 2. Filter holders
3. Reactor
4. Condensate trap
5. Isodiluter
6. Particle sensor
7. Particle counter
8. On-line printer

Figure 3.3 Outlet Sampling Sections

3.2 Equipment

To determine particle size distribution of the soot stream, a HAIC/ROYCO model 1200 aerosol sensor and microprocessor-based particle counter model 4100 was used. A HIAC/ROYCO D-50 Isodiluter was used in the particle sampling line, upstream of the particle counter.

3.2.1 Isokinetic Air Diluter D-50

The isokinetic air diluter model D-50 can provide a fixed and stable dilution of aerosol samples when the aerosol particle concentrations are near to or above the upper concentration limit of the particle counter. The nominal maximum concentration limit of particle counter model 4100/1200 without the isodiluter is about 100,000,000 particle/cubic foot. The model D-50 extends the concentration limit by a factor about 50. The effective dilution rate of the isodiluter is measured by determining how the concentration of particles change when the isodiluter is attached to the counter as shown in the data sheet in the Appendix A.1.

3.2.2 Aerosol Sensor Model 1200

The model 1200 aerosol sensor is an instrument for sensing particles in a gaseous media and developing a data signal to be used by the model 4100 particle counter. It is used typically in ambient air, in manufacturing installations, or in research laboratories. This model can count densities up to 100,000,000 particles per cubic foot. The particle size has to be equal to or larger than 0.5 μm. The operator selects the flow rate range of the

sample to be 0.1 cfm or 0.01 cfm by adjusting the switch at the front panel of the sensor. Time for each sample for the particle counter was 10 minutes.

3.2.3 Particle Counter Model 4100

The HYAC/ROYCO model 4100 is a microprocessor based particle counter which provides high-speed, precise particle size information on a wide variety of material suspended in liquid or air. It is able to acquire count data in 6 particle size ranges at the same time which can be independently set by the thumbwheel switches on the front panel. The particle counter was set to count 0.3, 0.4, 0.5, 0.6, 1.0, and 1.2 μm particle sizes. When the instrument is in the cumulative mode, each channel counts all particles larger than the threshold. In the differential mode each channel counts particles between the 2 adjacent thresholds. The operating procedure used for the Model 4100 is in the Appendix A.2.

3.3 Laser Measurement Technique

A Laser optical transmission method was developed and applied in order to measure the relative darkness of the soot density on the filter papers. The schematic of the apparatus is shown in Figure 3.4. The Helium-Neon laser light (632 nanometer wavelength) was steered by a mirror upward and through the filter paper sample held in a transparent petri dish. The amount of laser light which passed through the filter paper sample was collected by an amplified diode detector. This detector signal was measured in volts by a multimeter. Beam transmission through a completely white, clean filter paper was measured and used as the baseline. The detector gave the highest signal value for the

completely white, clean filter paper. Lower values of signal were obtained from the sample which were loaded with soot. The relative darkness of the samples were used as indicators of soot capture by the electrocatalytic reactor. The derivation of the relative darkness (% darkness) relation is in the Appendix B.

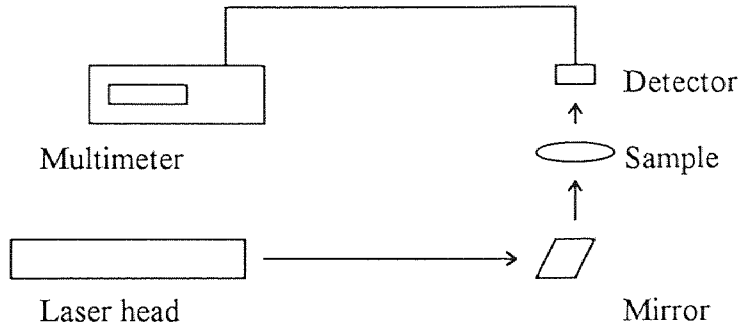

Figure 3.4 Schematic of The Laser Measurements

3.4 Experimental Programs

The experimental program can be separated into 5 phases in order to study the effects of the electrostatic forces, catalytic oxidation, and SOF content on soot capture by the electrocatalytic reactor.

1. Soot stream flowing through the reactor tube without added SOF and no external electric field. A blank tube was inserted into the reactor tube instead of a rolled catalyst material.

2. Soot stream flowing through the reactor tube with an external electric field. Instead of the rolled catalyst material, the blank tube was inserted in the reactor tube. SOF was not added in this experimental phase.

3. Soot stream flowing through the reactor tube with the catalyst material inserted in the reactor tube. External electric field was not applied in this phase. In addition, SOF was added in this experimental phase in order to determine the effect of adding vaporized toluene.

4. Soot stream flowing through the reactor tube with the catalyst material inserted in the reactor tube. External electric field was also applied in this phase. The temperatures in the reactor tube was set around 450 °C. In addition, SOF was also added in this experimental phase in order to determine the effect of adding vaporized toluene.

5. Soot stream flowing through the reactor tube with the catalyst material inserted in the reactor tube. External electric field was also applied in this phase. The temperature in the reactor tube was set around 520 °C.

CHAPTER 4

DEVELOPMENT OF MODEL EQUATIONS AND THE SOLUTION TECHNIQUES

4.1 Introduction

Deposition of charged particles in a circular straight tube without an applied electric field was studied by Chen (1978). In this chapter, the Chen equations are solved by a different numerical solution technique employing The Chebyshev Polynomial Software Package, PDECHEB, to predict the total deposition of charged particle in the circular straight tube. This numerical approach allows us to simulate the electrostatic and diffusional effects of lightly charged particles migrating to the wall in the straight tube reactor. There is no hydrodynamic mixing in this model. The velocity profile was assumed to be uniform in the radial direction, i.e., plug flow. A second model is presented which is a modification of the Deutsch equation. It is based on the existence of a turbulent well mixed core of uniform particle density. Unlike the Deutsch equation, the electric field in this case is due to the space charge from the charged particles in the reactor tube (i.e. no applied field). For both models, no applied field is present, and particle deposition on the surface of the wall is calculated as a function of axial distance in the tube. This work complements similar modeling studies by Callahan (1997) in which charged particles of different sizes flow through the reactor tube in the presence of an applied electric field.

4.2 Governing Equations from Chen (1978)

The basis for the steady-state governing equations used to simulate electrostatic and diffusional effects on the deposition on the wall of weakly charged particles in a circular straight tube is taken from Chen (1978). We consider that particles of uniform radius, a, and charge, q, flow through a circular reactor tube. The initial particle density at the entrance of the reactor, ρ_o, is assumed to be radially uniform. By symmetry of the circular tube, particle density at the center of the tube *(r=0)* is constant over an entire length of the tube*(x>0)*. Particle density at a wall *($\rho(R)$)* is assumed to be zero. These assumptions will be converted to boundary conditions in the following section. Chen also assumed that all particles were uniformly charged prior to entering a reactor tube. There is no hydrodynamic mixing in the tube.

The local electrostatic field resulting from the presence of the charged particles, is given by Poisson's equation as follows:

$$\frac{1}{r}\frac{\partial(re)}{\partial r} = \frac{\rho\, q}{\varepsilon_o} \qquad (4.2.1)$$

where ε_o is the permitivity of the air *($C^2/N\text{-}m^2$)*

r is a radial distance from the center line *(m)*

ρ is the particle density *(# particle/m^3)*

q is charge to mass ratio *(C^2/g)*

e is the local electrostatic field *(V/m)*

In Equation 4.2.1, the axial component of the electrostatic field has been neglected.

The transport equation for the steady state is given as follow:

$$u\frac{\partial \rho}{\partial x} = D\frac{1}{r}\frac{\partial}{\partial r}\left(\frac{r\partial \rho}{\partial r}\right) - \frac{1}{r}\frac{\partial}{\partial r}\left(\frac{rqe\rho}{6\pi\mu a}\right) \qquad (4.2.2)$$

where ρ is the particle density *(# particles/m^3)*

x is the axial distance measured from the inlet of the reactor tube *(m)*

D is the particle diffusivity *(m^2/s)*

μ is the viscosity of the gas *(N-s/m^2)*

a is a radius of the particle *(m)*

We have assumed plug flow, i.e., that the axial velocity (u) is independent of radial position. In Equation 4.2.2, the convection term is on the left hand side. The first term on the right hand side represents radial diffusion, and the second term on the right is due to the electrostatic flux. The system of equations (4.2.1 and 4.2.2) is the governing system of partial differential equations. A brief description of a solution technique which was employed to solve this equation system is found in the following section.

4.3 Chebyshev Polynomial Software for Solving the Partial Differential Equation System

The system of partial differential equations (PDEs) consisting of the particle transport equation and Poisson's equation for the electric field potential has been solved using PDECHEB, a package developed by Berzins and Dew (1991) for the numerical solution of parabolic-elliptic systems. It is a high-quality code which has undergone extensive testing on a full range of sample problems. This software automatically discretizes a spatial variable to give a system of ordinary differential equations (ODEs). In this application, the

radial variable, r, is discretized. The resulting ODE system is integrated with respect to the time-like variable, x, the axial distance along the reactor length. The discretization is accomplished using a piecewise polynomial approximant of the form $\sum a_i(x)T_i(r)$, where $T_i(\cdot)$ is the Chebyshev polynomial of the first kind of degree i. In the derivation of the algorithm, this approximant is substituted into the partial differential equations and the resulting relations are required to hold at a set of points which are the roots of the appropriate Chebyshev polynomial. The software thus achieves spatial discretization by the method of orthogonal collocation. The resulting system consists of both differential and algebraic equations. The widely used differential-algebraic system solver DASSL (Petzold et al., 1989) was employed for the x-integration.

In order to use this software, it was necessary to code a driver in FORTRAN which initializes PDECHEB and repeatedly calls DASSL to integrate with respect to x. The system of PDEs and the boundary and initial conditions are specified by writing three subroutines in the required PDECHEB format. Values for the operating parameters (e.g., flow rate, reactor length, particle size) are read from a user-supplied input file. The output consists of the radial profiles of particle density and electric field potential at the indicated value of x. These value were also written to a data set in a form suitable for subsequent plotting.

The following dimensionless quantities are introduced for Equations 4.2.1 and 4.2.2.

$$R = \rho/\rho_o \qquad r^* = r/r_o \qquad U = u/u_o$$

$$X = xD/r_o^2 u_o \qquad E = qr_o e/6\pi\mu a D \qquad \alpha = \rho_o q^2 r_o^2/24\varepsilon_o D\pi\mu a$$

where α is a dimensionless charge parameter

r_o is a radius of the reactor tube *(m)*

u_o is the mean velocity of flow *(m/s)*

ρ_o is a uniform particle density at the entrance of the reactor tube *(# particles/m^3)*

After applying the dimensionless quantities, Equations 4.2.1 and 4.2.2 become :

$$\frac{1}{r^*}\frac{\partial(r^*E)}{\partial r^*} = 4\alpha R \qquad (4.3.1)$$

$$U\frac{\partial R}{\partial X} = \frac{\partial}{r^*\partial r^*}\left(r^*\frac{\partial R}{\partial r^*} - r^*RE\right) \qquad (4.3.2)$$

As mentioned in section 4.2, the boundary conditions are

$R = 1$ *at* $X = 0$ *for all* r^*

$\partial R/\partial r^* = E = 0$ *at* $r^* = 0$ *for* $X > 0$

and $R = 0$ *at* $r^* = 1$ *for* $X > 0$

Equations 4.3.2 and 4.3.3 need to be written in the PDECHEB form (Berzins and Dew, 1991) in order to be solved by the program. Rearranging Equations 4.3.1 and 4.3.2 results in the following equations:

$$4\alpha R = \frac{1}{r^*}\frac{\partial(r^*E)}{\partial r^*} \qquad (4.3.3)$$

$$U\frac{\partial R}{\partial X} = \frac{\partial}{r^*\partial r^*}\left(r^*\frac{\partial R}{\partial r^*} - r^*RE\right) \qquad (4.3.4)$$

4.4 Derivation of a Modified Deutsch Equation for Turbulent Plug Flow with Field due to Charged Particles

Derivation of the basic transport and the Deutsch equations is the second modeling effort to understand characteristics of the soot particles in the reactor tube. As opposed to Chen plug flow studies in which there was no hydrodynamic mixing, axial turbulent flow is assumed to produce a radially uniform particle density core, in effect, plug flow. Particle transport to a wall is dominated by the electrostatic particle flux from the field due to charged particles (space charge). As shown in Figure 4.1, a volume increment is well mixed, so particle density in the gas stream is a function of x alone.

A general particle mass balance equation at steady state is given across a differential volume as follow:

{flow in} - {flow out} = { rate of particle deposition on the tube wall}

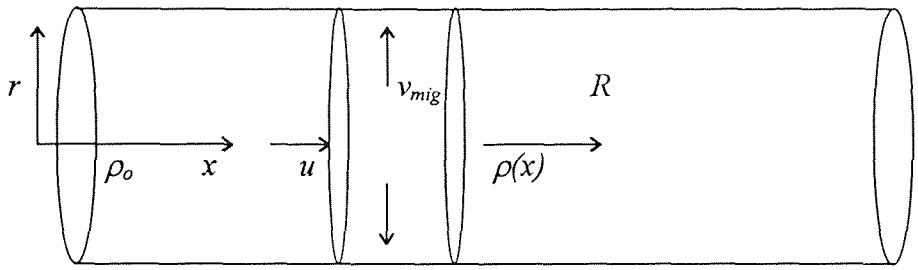

Figure 4.1 Mass Balance Across a Differential Volume in a Reactor Tube

flow in $= Au\rho(x)$

flow out $= Au\rho(x+\Delta x)$

rate of deposition on a tube wall in the differential volume $= \rho(x)v_{mig}2\pi R\Delta x$

where A = cross section area of the reactor tube (m^2)

R = inside tube radius (m)

v_{mig} = soot particle velocity in the radial direction to the wall *(m/s)*

Then the general mass balance becomes

$$Au\rho(x) - Au\rho(x+\Delta x) = \rho(x)v_{mig}2\pi R\Delta x \qquad (4.4.1)$$

Migration velocity to the wall was derived from Strokes' drag force due to electric field:

$$v_{mig} = \frac{qe}{6\pi\mu a} \qquad (4.4.2)$$

The field due to the charged particle (space charge) is given by Poisson's equation:

$$\frac{1}{r}\frac{\partial(re)}{\partial r} = \frac{\rho q}{\varepsilon_o} \qquad (4.4.3)$$

After integrating with the boundary condition $\frac{\partial e}{\partial r} = 0$, we get

$$e = \frac{\rho q r}{2\varepsilon_o} \qquad (4.4.4)$$

Thus, e at the wall of the reactor tube can be expressed as:

$$e\,/_{r=R} = \rho qR/2\varepsilon_o \qquad (4.4.5)$$

By substituting Equation 4.4.5 in Equation 4.4.2

$$v_{mig} = \frac{q^2 R\rho}{12\pi\mu a\varepsilon_o} \qquad (4.4.6)$$

By substituting v_{mig} from Equation 4.4.6 in Equation 4.4.1, then dividing through by πR^2, then let $\Delta x \rightarrow 0$, the above equation becomes in differential form:

$$u\frac{d\rho}{dx} + \frac{q^2\rho^2}{6\pi\mu a\varepsilon_o} = 0 \qquad (4.4.7)$$

Non-dimensional quantities are introduced :

$\rho^* = (\rho/\rho_o)$ $\qquad$ $X^* = xD/R^2u_o$

Then, Equation 4.4.7 can be written as follow:

$$\frac{d\rho^*}{dX^*} + 4\alpha\rho^{*2} = 0 \qquad (4.4.8)$$

where $\alpha = \rho_o q^2 R^2 / 24\varepsilon_o D\pi\mu a$ which is the same α in section 4.3.

The result after integration of Equation 4.4.8 is as follows:

$$\rho^* = \frac{1}{4\alpha X^* + C_1} \qquad (4.4.9)$$

From the boundary condition : $\rho^* = 1$ at $X^* = 0$, it follows that $C_1 = 0$. Hence,

$$\rho^* = \frac{1}{4\alpha X^* + 1} \qquad (4.4.10)$$

4.5 Results and Discussions

In this analysis, the particle diameter was assumed to be 1 μm. This average number came from the results from the particle counter and studies of soot particles in the past (Aldersey, 1989; Ciambelli, 1990; Chung, 1991; Thimsen, 1990; Callahan, 1997). The dimensionless charge parameter (α) for an inlet particle density of 1.5×10^6 particle/m^3 (Callahan, 1997) ranged from 5-100. Figure 4.2 shows the penetration in a tube for plug flow at various values of the dimensionless charge parameter (α) by employing the PDECHEB numerical method to Equations 4.3.4 and 4.3.5. The results from Chen (1978) are also shown in Figure 4.3 for the penetration in a tube. In this study, penetration in the reactor tube is defined as a particle density at a specific point, $\rho(x)$, divided by an inlet particle density, ρ_o. Comparison of the present results (Fig. 4.2) with those in Figure 4.3 by Chen indicated that the results obtained by employing PDECHEB numerical method agree with those presented by Chen (1978). Both figures clearly show the effect of the

dimensionless charge parameter (α) on soot capture in the reactor tube. From both figures, higher dimensionless charge parameters (α) resulting in higher soot capture effectiveness in the tube.

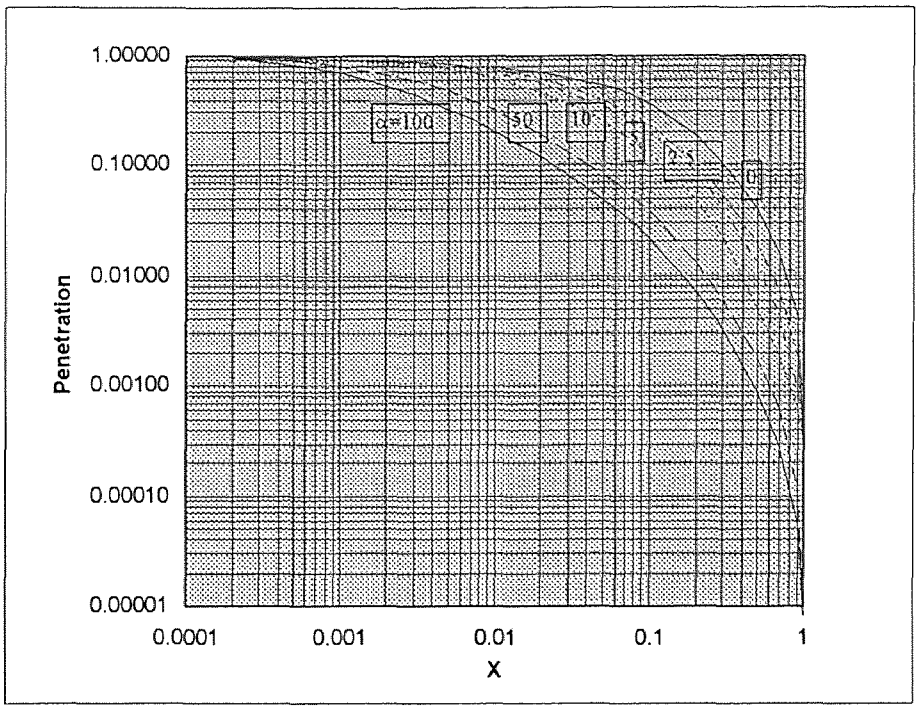

Figure 4.2 Penetration in a Tube by Employing PDECHEB Numerical Technique

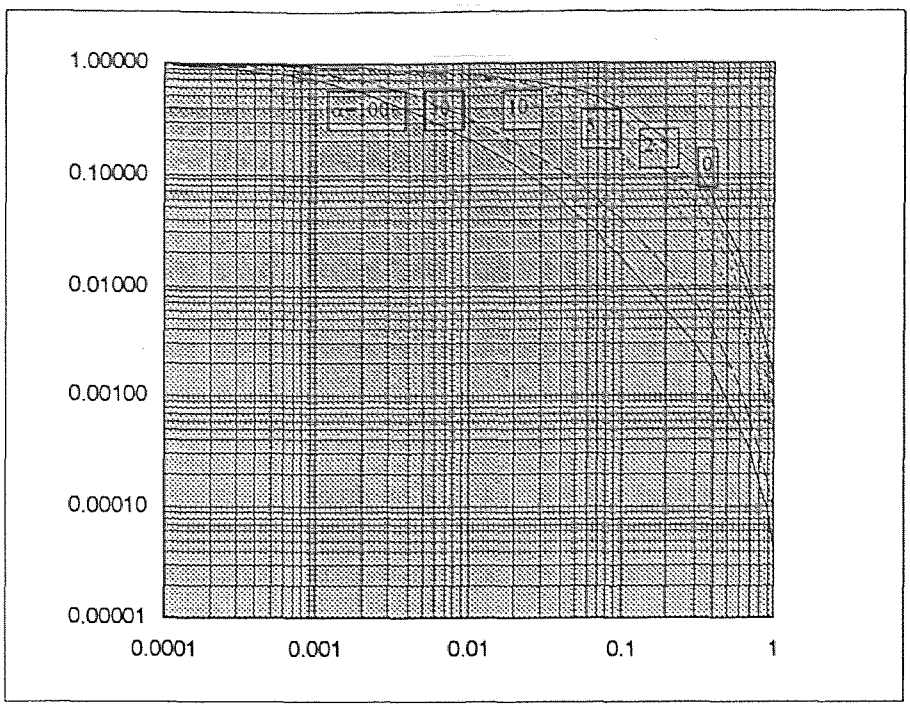

Figure 4.3 Penetration in a Tube by Employing an Integral Method (Chen 1978)

Figure 4.4-4.8 show the penetration of charged particles in a reactor tube at various dimensionless charge parameters (α). The solid lines represent the modified Deutsch model (Equation 4.4.10). The dotted-lines represent the Chen model (Equations 4.3.4 and 4.3.5) which was solved by using the PDECHEB software package as mentioned earlier in section 4.3. These figures clearly show that the penetration for both cases have similar trend almost the entire axial length of reactor. However, the model with no hydrodynamic mixing (Chen) indicates higher efficiency soot capture than the turbulent plug flow model (modified Deutsch). These results support idea that with turbulent plug flow, there is a tendency for some particles near the tube wall to be brought back into the center core of the tube, thus lowering particle deposition on the wall, or increasing particle penetration. Furthermore, the results from Figure 4.4-4.8 also represent limiting cases of

no hydrodynamic mixing and a complete turbulent (well mixed) core. The results suggest that a model for a real system might lie between these two cases

The most important thing of all is the non-dimensional X value. The non-dimensional value for the actual reactor tube length (40 cm) is approximately 10^{-8} which is very small number. The model show no significant change for the penetration in the reactor tube at such a small non-dimensional X value. At this range of non-dimensional X value, almost any soot particles which go into the reactor tube can penetrate through the exit of the tube. Indeed, soot particles are hardly captured in the actual reactor tube without an external electric field, as will be shown in chapter 5.

The effects of electrostatic precipitation through the use of a central wire has been investigated by Callahan (1997). Comparing the present results to his study, the external electric field generated by the use of a central wire has a major effect on the soot capture in the reactor tube. The presence of a strong applied field dominates any effect due to the field causing from the charged particle.

The study of multifractional size particle deposited in the reactor with an external applied field in the turbulent flow region has not been included in this study. It would be interesting to extend the present method to include such conditions in the future.

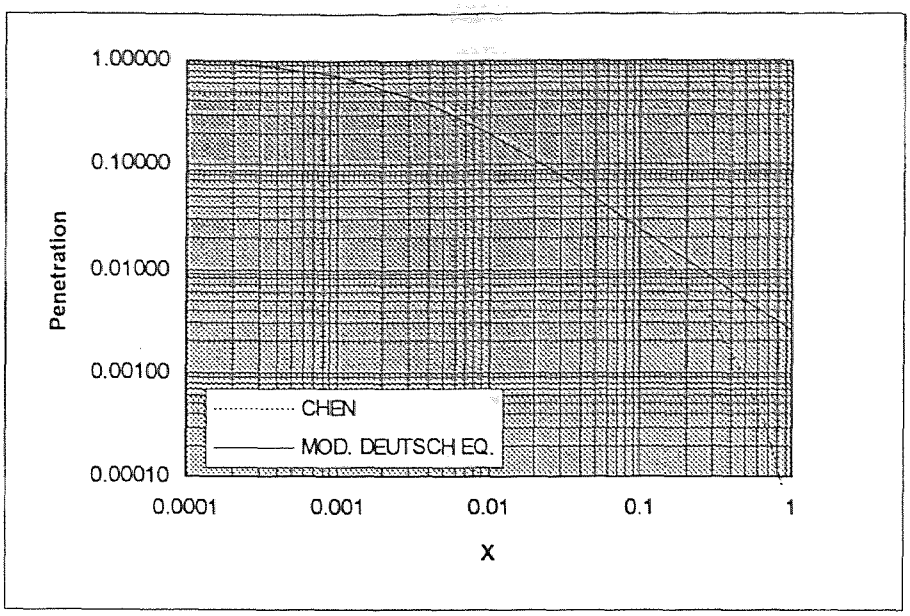

Figure 4.4 Penetration in a Tube for Alpha (α) = 100

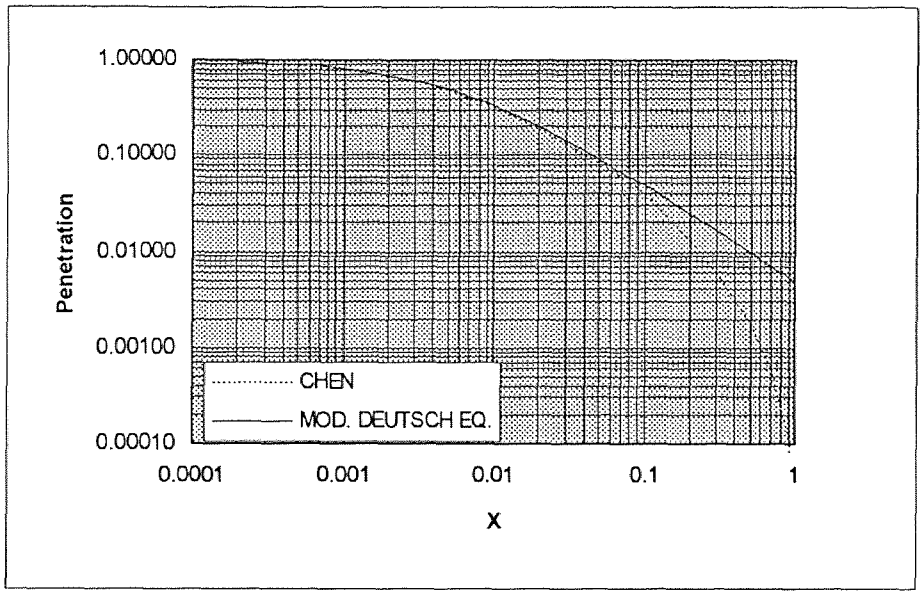

Figure 4.5 Penetration in a Tube for Alpha (α) = 50

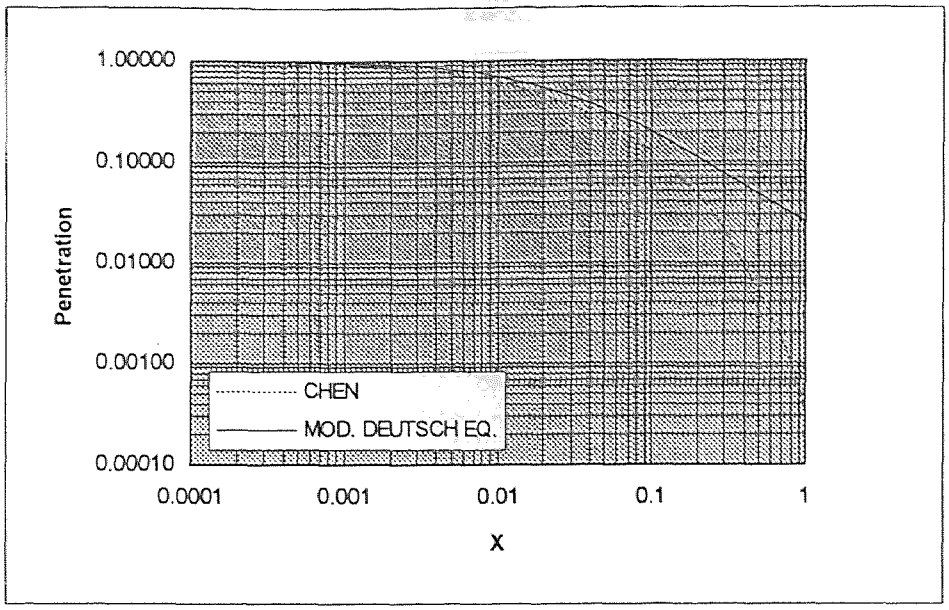

Figure 4.6 Penetration in a Tube for Alpha (α) = 10

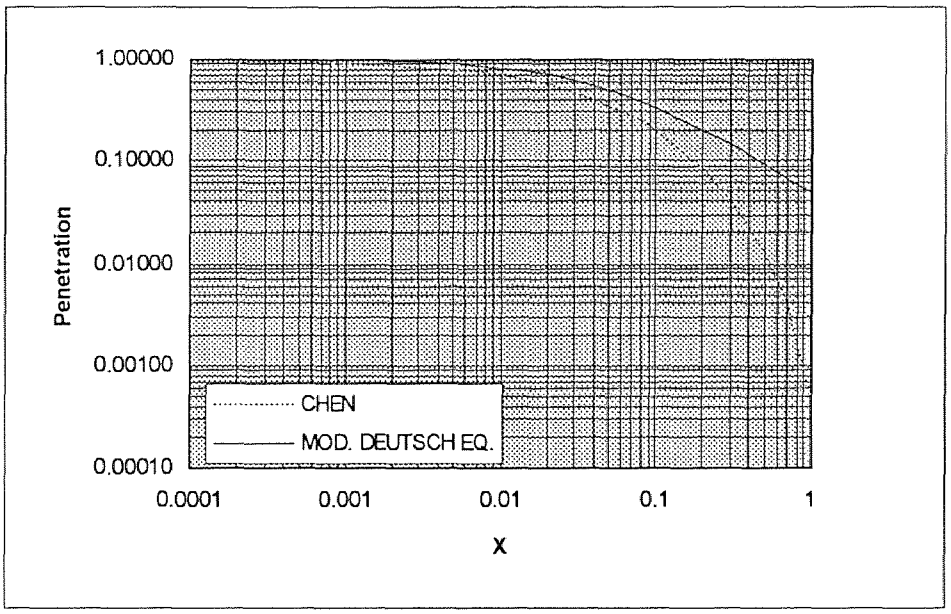

Figure 4.7 Penetration in a Tube for Alpha (α) = 5

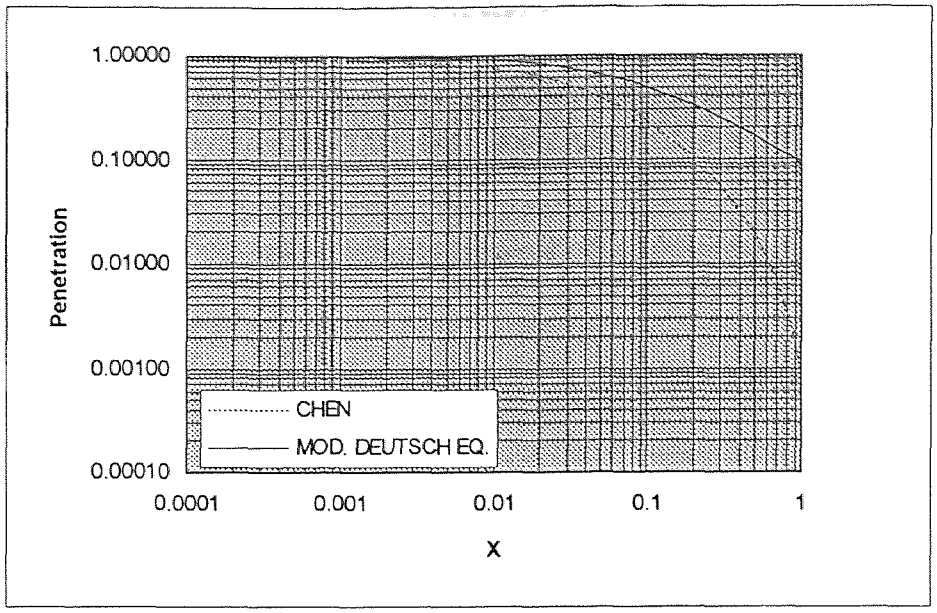

Figure 4.8 Penetration in a Tube for Alpha (α) = 2.5

CHAPTER 5

RESULTS AND DISCUSSIONS

5.1 Experiments Using a Blank (Non-Catalytic) Tube without an Applied Field

This set of experiments was performed by inserting a stainless steel blank tube into the reactor tube instead of the rolled catalyst material. The objectives here were design to ensure that the filter paper sampling system of both inlet and outlet worked properly, as well as to determine the amount of soot that flowed into and out from the blank tube. By the visual inspection, a uniform and light coating of soot was found inside the blank tube.

The outlet filter samples were slightly lighter than those of in the inlet, which indicated the dilution effect caused by the injected O_2 as expected. The weight gain due to soot deposition for inlet filter paper samples were about the same as for the outlet filter paper samples (0.1-0.5 milligrams). Because the weight gains were so small, and were at the sensitively limit of the scale, the gravimetric data were inconclusive.

The particle counter was set to count 0.3, 0.4,0 0.5, 0.6, 1.0, and 1.2 μm particle sizes. The time set for each sample on the particle counter was 10 minutes. The total cumulative count for each sampling was about 50,000. The counts were significantly high at the 0.3 μm particle size. This is the lowest size range of the particle counter; therefore, counts in this region are suspect.

For the rest of the experimental program, no matter when the voltage was applied or the roll catalyst material was inserted, the results of the weight gain and the results from the particle counter were not that different from this set of experiments. This suggested that another analysis technique was necessary to distinguish true results from background noise.

5.2 Experiments Using a Blank (Non-Catalytic) Tube with an Applied External Field

The purpose of this set of experiments was to study the effects of an electrostatic precipitation without the catalyst material. Various voltages from the DC power supply were applied (500, 1000, 1500, ... 3500 volts). Inlet and outlet samples were taken by using the filter paper samplings. Inlet samples were taken in order to ensure that a suitable amount of soot went into the reactor tube as well as to check whether the combustor worked consistently with no significant drift over time. There were no significant changes in the inlet filter paper samples even when various voltages were applied, which showed the consistency of the system.

The outlet filter paper samples grew lighter as the voltage was increased, which definitely showed the soot capture effect of electrostatic precipitation. Agglomerated soot was also found on the outlet filter paper when the voltage was applied. The agglomerated soot appeared as tiny black spots all over the filter paper as well as at the exit of the reactor tube. The agglomerated soot was easier to notice especially when the high voltage was applied. This observation is consistent with the previous studies by Kittelson (1991). The last observation from this set of experiments was that a good coating of soot was found inside the blank tube . This soot coating was heavier than the one in the previous set of experiment, showing an impact of the applied external field which definitely helps driving soot particles to the wall.

5.3 Experiments Using the Catalyst Material without an Applied External Field

The purpose of this set of experiments was to study the impact on soot capture of the catalyst surface only. The rolled catalyst sheet was inserted in the reactor tube instead of the blank tube. For each run, the first set of samples, filter paper and GC samplings (Callahan 1997), were taken both at the inlet and outlet. After the first sample set was completed, pure oxygen gas was added into the reactor tube. At this time, the second sample set was taken. The last sample set was taken after the vaporized toluene (SOF) was added while the pure oxygen was still on.

Originally, the tube furnace controllers were set at 400 °C. Catalyst surface temperatures increased about 15-30 °C when oxygen was added which indicated catalytic oxidation of soot occurring on the catalyst surface. Oxygen flow rate was 5.1 litr/min.. However, there was no significant change after SOF was added, which suggested SOF does not have any effect on the catalytic oxidation as originally thought.

The outlet filter paper samples were slightly lighter than those of the inlet because of the dilution effects as mentioned in section 5.1. Figure 5.1 showed a comparison of a darkness between inlet and outlet filter paper samples for some runs. Beyond dilution, outlet filter samples showed little or no decrease in soot loading as compared to inlet samples. All outlet filter samples were similar to one another. The result suggests that catalytic oxidation, without electrostatic precipitation, has a minor effect on soot capture in the reactor tube. These results, and the results from section 5.2, are consistent with the modeling results from chapter 4 which indicated that the external electric field generated by the use of a central wire has the major effect on soot capture in the reactor tube. The

external field effect predominates over any precipitation due to particle charges resulting from the combustion process prior to entering the reactor tube (i.e. no applied field).

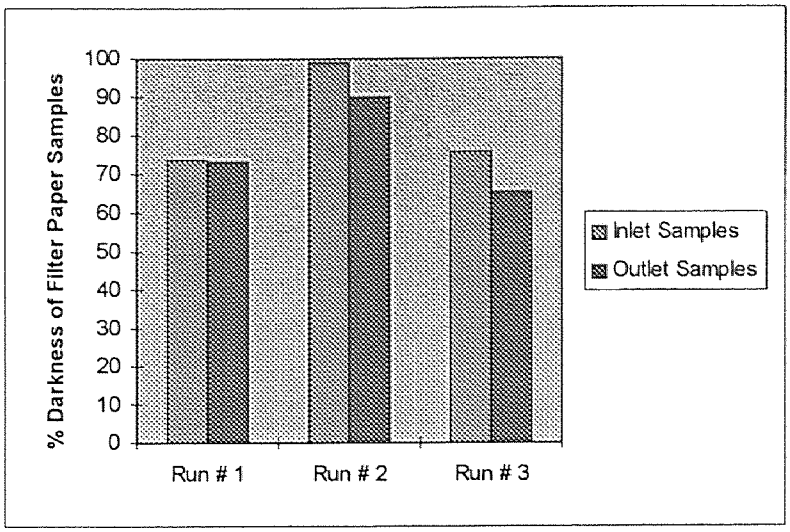

Figure 5.1 Darkness Comparison between Inlet and Outlet Filter Paper Samples

5.4 Experiments Using the Catalyst Material with an Applied External Field at 450 °C in the Reactor Tube

In these experiments, the tube furnace controllers were set at 450 °C. The outlet filter paper samples showed a significant decrease in darkness, with very small agglomerated particles on the filter paper when high voltage was reached (3500, 4000, ..., 5000 volts). Figure 5.2 shows the soot penetration, based on laser analysis of filter paper samples, under various voltages, and under fairly heavily sooting conditions. The y-axis (penetration) represents the darkness ratio or the darkness of each sample divided by the darkness of a reference inlet sample. As shown in the figure, there is no significant change until a voltage of 3500. The lowest value of the darkness ratio, representing percent soot

capture, was obtained at 5000 volts, definitely showing the effects of the electrostatic precipitation.

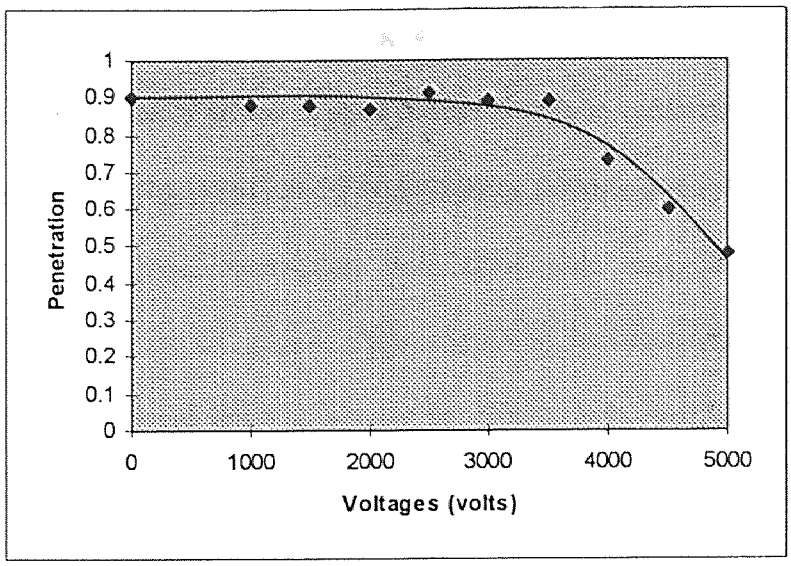

Figure 5.2 Penetration in a Tube at Lower Temperature under Various Voltages

Catalytic oxidation was not apparent at high voltages (greater than 3500 volts) because a heavy coating of soot on the catalyst surface. The velocity of the soot laden stream in the reactor tube was around 350-450 ft/min. The temperatures along the reactor tube increased just slightly (about 5°C) after oxygen (5.1 litr/min.) was added. These temperature increase was less than the increase seen in the previous set of experiments (no applied field). Apparently, at high voltages, soot is so well driven to the wall that the catalyst can not function since it is too heavily covered.

SOF was also added to the reactor tube feed. It still did not appear to have any effect on the reactor tube temperatures as well as on CO_2 and CO levels which were

detected by GC (Callahan 1997) . This suggested that adding vaporized toluene into the catalytic reactor tube does not enhance catalytic oxidation as original suggested.

When O_2 was increased from 5.1 litr/min. to 9.2 litr/min., catalyst surface temperatures increased about 20-30°C, suggesting that catalytic oxidation of soot was occurring. The importance of added oxygen observed here is consistent with the previous studies by Chung and Tsang (1991) and The Society of Automotive Engineers (1983).

The most important observation from these data and the data from visual inspection, together with the GC data of Callahan (1997), was that when high voltage was reached, CO and CO_2 level did not appear to differ much, suggesting that the soot oxidation efficiency of the electrocatalytic reactor diminished. At the high voltage, it appears that the rate of the soot which was driven to the wall was much higher than the catalytic oxidation rate on the rolled catalyst surface. Thus, a thick layer of the soot built up on the catalyst wall, prevented the oxygen from getting through the catalyst surface to provide catalytic oxidation.

Visual inspection revealed that the center wire had a coating of soot on it. This observation suggested that soot particle might be a bi-polar charged, and that causing some positive charged accumulation on the negative wire.

The study of adding vaporized toluene (SOF) into the reactor tube was terminated by the end of this experimental set because no significant impact had been found in any run after adding vaporized toluene into the catalytic reactor tube. A more encouraging result turned out to be the impact of oxygen which was added into the reactor tube, and also the surface temperature of the rolled catalyst material.

5.5 Experiments Using the Catalyst Material in the Reactor Tube with an Applied External Field at 500 °C in the Reactor Tube

The tube furnace controllers were set to 500 °C for this set of experiments. This was about 50 °C higher than the previous experimental set. Both the low flow and the high flow of added oxygen were tested. The results of filter paper samplings were similar to the experiment in section 5.4. Figure 5.3 shows soot penetration with increasing voltages under a light soot condition. The drift of the curve at 5000 volts was caused by a difficulty controlling the sampling flow rate before the end of the experiment. The agglomerated particles on the filtered paper could still be noticed when high voltage was reached. Both Figure 5.2 and Figure 5.3 show a drop in penetration after 3500 volts. Lower penetrations were observed at the higher tube temperature.

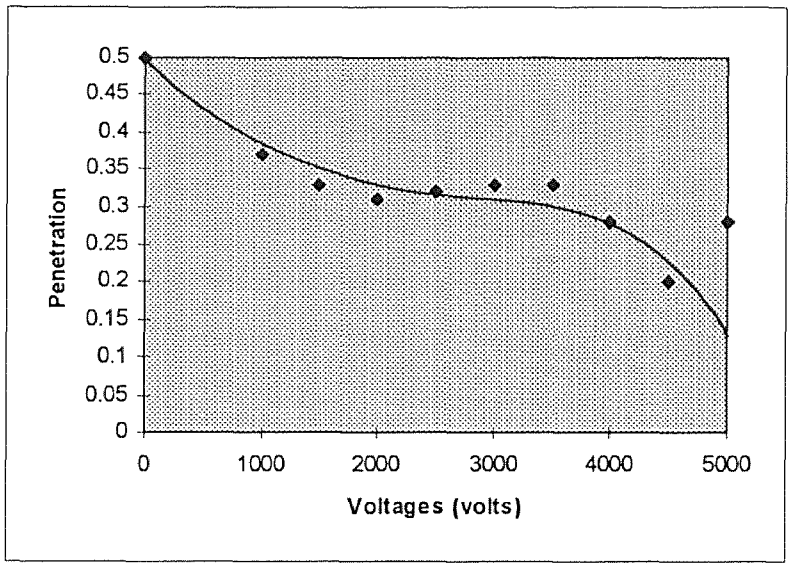

Figure 5.3 Penetration in a Tube at Higher Temperature under Various Voltages

Increasing temperature in the reactor tube caused the soot laden stream velocity in the reactor tube became around 500-600 ft/min., higher than the previous set of experiments.

There was no evidence of increasing temperature of the surface of the rolled catalyst material after adding oxygen either at the smaller flow or higher flow. There are two possible explanations. One is permanent loss of catalyst activity. This catalyst roll had been in use since the very beginning of this research study. The second assumption is that the heat which generated from the catalytic oxidation of soot might be removed by the higher gas flow in the reactor tube. If the latter assumption is true, it will be consistent with the previous studies by Chung and Tsang (1991). Accumulated soot on the central wire was still found as in the previous set of experiments.

CHAPTER 6

CONCLUSIONS

The results obtained through this investigation can lead to the following conclusions:

1. Soot plugging problem can be alleviated by using a large flow channel reactor instead of a small monolith.

2. Electrostatic precipitation through the use of a central wire showed a significant effect on soot capture in a reactor tube. Higher voltages resulting in lower outlet soot concentrations.

3. The system effectiveness at low voltages was a combination of the electrostatic precipitation and catalytic oxidation. Reactor outlet soot concentrations showed a significant decrease when high voltages was applied, showing a strong effect of the electrostatic precipitation. However, catalytic oxidation was not apparent at high voltages because a heavy coated of soot was found on the catalyst surface.

4. Results from visual observation and GC samples (Callahan 1997) suggest that, at high voltages, the rate of the soot which was driven to the wall was much higher than the catalytic oxidation rate. Therefore, a thick layer of soot was built on a rolled catalyst material, preventing the oxygen from getting through the catalyst surface to initiate catalytic oxidation.

5. The soot capture results are consistent with the present simulation models and the modeling results investigated by Callahan (1997).

APPENDIX A

A.1 MODEL D-50 ISODILUTER QC DATA SHEET

IsoDiluter Serial Number *95100197* Date: *10/13/95*
Technician
Measure Performance (Cumulative Counts per Cubic Foot, i.e. " Normalized")
Counter Model *5230* Counter Serial Number *Plant STD*

Sample Run #*1/2*	>0.5	>1.0	>2.0
Not Installed	*12228*	*1920*	*459*
Installed	*400*	*92*	*48*
Ratio	*30.57*	*20.86*	*9.56*
Sample Run #*5/6*	>0.5	>1.0	>2.0
Not Installed	*12873*	*2188*	*551*
Installed	*251*	*38*	*6*
Ratio	*51.28*	*57.57*	*91.83*
Sample Run #*9/10*	>0.5	>1.0	>2.0
Not Installed	*15747*	*2419*	*538*
Installed	*284*	*45*	*12*
Ratio	*55.44*	*53.75*	*44.83*
Average Ratio	*45.76*	*44.06*	*48.74*

Average of 0.5, 1.0, and 2.0 ratios *46.18*

Check sheet :: __ Dilution Ratio is between 7.5 and 12.5 (Model D-10)

√ Dilution Ratio is between 37.5 and 62.5 (Model D-50)

√ Dilution Ratio is written on the label

√ Tubing is tied down (if applicable)

A.2 OPERATING PROCEDURE FOR MODEL 4100

1. Turn on power by pressing the power toggle switch on the rear panel to *ON*. Allow 8 second for self-testing and then a printer, connected to the particle counter prints out the following:

```
**********
HIAC/ROYCO
**********
11/01/96      10:10:20
SELF TEST RESULTS
  CHECKSUM  OK
  RAM TEST   OK
  BATTERY RAM  OK
  BATTERY TEST  OK
  CLOCK RUNNING
```

If any of the self-test fail, the model 4100 will send out a warning signal by flashing the *SYSTEM FAIL LED*.

2. The series of channel threshold thumbwheels should be set to correlate the selected particle size thresholds with the calibration curve for the sensor model 1200 that being use. Operator has to arrange the threshold size in progressive order, so that channel 1 has the lowest setting and channel 6 has the highest.

3. Adjust the sampling time.

4. Press *START* to start run, the counter will automatically stop when it come to the setting time.

APPENDIX B

B.1 THE DERIVATION OF THE RELATIVE DARKNESS FOR THE LASER MEASUREMENT

1. Detector baseline (*A volts*) is the default value of the detector. This is the lowest value which we can obtain from the detector.

2. For the completely white, clear filter paper, *B* volts($B>A$) is the value which is obtained from the detector. This value is the highest value for the measurement

3. *C* volts is the detector range which equals ($B-A$)

4. *D* is the value and obtained from the detector for the sample we want to measure

5. $A \leq D \leq B$

6. *E* is the relative darkness (*% darkness*)

$$E = \{C-(D-A)\}\times 100/C \quad \%$$

Example 1

Detector baseline = *33.15*

Detector read for a completely white, clean filter paper = *35.0*

$\therefore$ Detector range = *35.0-33.15*

= *1.875*

Raw data

	Detector read value	Remarks
Sample # 1	*34.8*	*Very light soot, the color of the sample is almost white*
Sample # 2	*34.0*	*The color of this sample is slightly darker than Sample#1*
Sample # 3	*33.8*	*The color of this sample is slightly lighter than Sample#4*
Sample #4	*33.2*	*Heavily laden with soot, the color of the sample is almost black*

For sample # 1

Relative darkness = *{1.875-(34.8-33.15)}×100 / 1.875*

= *12.00 %*

For sample # 2

Relative darkness = *{1.875-(34.0-33.15)} ×100 / 1.875*

= *54.66 %*

For sample # 3

Relative darkness = *{1.875-(33.8-33.15)}×100 / 1.875*

= *77.47 %*

For sample # 4

Relative darkness = *{1.875-(33.2-33.15)}×100 / 1.875*

= *97.30 %*

Then the results from the measurment are as follows:

	Detector read value	**Realative Darkness(%)**
Sample # 1	*34.8*	*12.00 %*
Sample # 2	*34.0*	*54.66 %*
Sample # 3	*33.8*	*77.47 %*
Sample #4	*33.2*	*97.30 %*

REFERENCES

Ahlstrom, A. Fredrik and C.U. Ingemar Odenbrand. "Catalytic Combustion of Soot Deposits from Diesel Engines." *Applied Catalysis*. v80, (1990): 143-156.

Berzins, M., P.M.Dew. " Algorithm 690 Chebyshev Polynomial Software for Elliptic-Parabolic System of PDEs." *ACM Transactions on Mathematical Software. v17*, No.2, (1991): 178-206.

Brenan, K.E., Campbell, S.L. and Petzold, L.R. *Numerical Solution of Initial Value Problems in Differential-Algebraic Equations* North Holland, Amsterdam, 1989.

Caruana, M. Claudia. "Dutch Give a Delft Touch to ChE Research." *Chemical Engineering Progress*. v87, (1991): 8.

Chen, R.Y. " Deposition of Charged Particles in Tubes." *Journal of Aerosol Science*.v9, (1978): 449-453.

Chin, J. S. and A. H. Lefebvre. " Influence of Fuel Chemical Properties on Soot Emissions from Gas Turbine Combustors." *Combustion Science and Technology*. v73, No. 1-3, (1990): 479-486.

Chung, Shyan-Lung and Sheung-Man Tsang. "Soot Control During the Combustion of Polystyrene." *Journal of the Air & Waste Management Association*. v41, (1991):821-826.

Ciambelli, P., P. Corbo, P. Parrella, M. Scialo, and S. Vaccaro. " Catalytic Oxidation of Soot From Diesel Exhaust Gases." *Thermochimica Acta*. v162, (1990): 83-89.

Cooper, J. Barry, Hyun J. Jung, Janes E. Thoss. "Sweeping the Soot from Dirty Diesel." *Chemistry and Industry*, No.4, (1995):121.

Doorn, J. van, J. Varloud, P. Meriaudeau, and V. Perrichon. "Effect of Support Material on the Catalytic Combustion of Diesel Soot Particulates." *Applied Catalysis B; Enviromental*. v1, (1992): 117-127.

Fogler, H. Scott. *Elements of Chemical Reaction Engineering*. 2nd ed. New Jersey: Prentice-Hall, 1992.

Himes, R. M., R. L. Hack, G. S. Samuelsen. " Chemical and Physical Properties of Soot as a Function of Fuel Molecular Structure in a Swirl-Stabilized Combustor." *Journal of Engineering for Gas turbines and Power*. v106, (1984): 103-108.

REFERENCES
(Continued)

Khalil, Najib and Yiannis A. Levendis. " Development of a New Diesel Particulate Control System with Wall-Flow Filters and Reverse Cleaning Regeneration." *SAE Transactions, Journal of Engines*. v101, No. 3, (1992): 985-999.

Kittelson, David B. and David Y.H. Pui. "Electrostatic Collection of Diesel Particles." *SAE Transactions*. v95, No. 1, (1986): 51-61.

Ludecke, Otto A. and Kenneth B. Bly. "Diesel Exhaust Particulate Control by Monolith Trap and Fuel Additive Regeneration." *SAE Transactions*. v93, No. 1,(1984): 444-451.

Mitchell, J. B. A., D. J. M. Miller, and M. Sharpe. "The Use of Additives in the Control and Elucidation of Soot." *Combustion Science and Technology*. v74, No.1-6, (1990):63-66.

Patel, Kam. "Ford Aims for a Lead in Cleaner Diesel Exhausts." *The Engineering (London, England)*. v273, (1991): 36.

Shadman, F. . "Kinetic of Soot Combustion During Regeneration of Surface Filters." *Combustion Science and Technology*. v63, No. 4-6, (1989): 183-191.

Society of Automotive Engineers, Inc.."Air Cell Combustion Chamber Reduces Diesel Soot." *Automotive Engineering*. v91, (1983): 51-52.

Thimsen, David P. , Kirby J. Baumgard, and Thomas J. Kotz. " The Performance of an Electrostatic Aggromerator as a Diesel Soot Emission Control Device." *SAE Transactions, Journal of Engines*. v99, No. 3, Part 1,(1990): 728-737.

Yuan, Shibin, Paul Meriaudeau, and Vincent Perrichon. "Catalytic Combustion of Diesel Soot Particles on Copper Catalysts Supported on TiO_2; Effect of Potassium Promoter on the Activity." *Applied Catalysis B; Environmental*. v3,(1994): 319-333.